

Simultaneous B_0 and High Dynamic Range B_1 Mapping Using an Adiabatic Partial Passage Pulse

K. Shultz¹, G. Scott¹, J. Barral¹, and J. Pauly¹

¹Electrical Engineering, Stanford University, Stanford, CA, United States

Introduction: Many B_1 mapping sequences, such as the double angle method (DAM) [1] or actual flip-angle imaging (AFI) [2], only cover a limited dynamic range (approximately a factor of 2 between the largest and smallest $|B_1|$ that can be resolved) and do not measure B_0 . Many situations where B_1 mapping is necessary have a large range of $|B_1|$ and B_0 variation. Surface coils, such as those used for parallel transmit, and current-carrying wires, such as those used in RF ablation, can have an order of magnitude or more variation in field strength. Air/tissue interfaces, different chemical species and the presence of metal wires create off-resonance, which can lead to image distortion when using long readouts. Techniques like the DAM or AFI can be extended to a larger dynamic range through multiple repetitions with different excitation magnitudes, but the extended range comes at a cost of increased scan time and increased reconstruction complexity. We present an adiabatic partial passage (APP) B_1 mapping sequence that covers a 16-fold dynamic range while simultaneously mapping B_0 field variations.

Theory: If an adiabatic pulse is not brought all the way to on-resonance, the angle of the effective field, and therefore the flip angle of the magnetization, will be dependent on the magnitude of B_1 . This is an adiabatic partial passage (APP) as opposed to the typical adiabatic half or full passage. A second partial passage pulse with the opposite sign of frequency offset compensates for deviation from the theoretical tip angle due to external off-resonance. By using a full adiabatic half passage as a reference 90° excitation, the variation in B_1 can be measured [3]. Due to the length of the adiabatic pulse, relaxation will occur during excitation. In order to account for the different relaxation due to the shorter length of the partial passage pulses, the delay until data acquisition is referenced from the beginning of each pulse. This increases TE for the partial passage excitation, so a B_0 map can be created by comparing the phase of the acquisitions.

Methods: Two experiments were performed to compare our APP B_1 mapping sequence to the standard double angle method (DAM). For the DAM, 5 amplitudes of B_1 were used, doubling the magnitude with each acquisition, to cover the same 16X dynamic range as the APP sequence. The adiabatic pulse is a modified sech/tanh pulse, adapted using the method of Ugurbil et al [4] to cover a 16X dynamic range of $|B_1|$ and ± 400 Hz ΔB_0 . Both sequences used an adiabatic reset pulse after acquisition to reset the magnetization [5]. Images were acquired on a 1.5 T GE Signa scanner.

Off-resonance experiment: A 1-inch diameter transmit/receive surface coil was used to image a phantom consisting of water doped with 2.5 mM NiCl_2 . The shim in the y-dimension was set to create ± 220 Hz inhomogeneity in B_0 across the phantom. No other shims were applied so additional field variation was present. Both sequences used a 3D stack-of-EPI readout with 16 echoes, TR = 1 s, $0.9 \times 0.9 \text{ mm}^2$ in-plane resolution and 2 mm slice thickness. The scan times were 10 minutes for the DAM and 6 minutes for the APP sequence.

Wire experiment: A wire acted as a transmit/receive element to simulate a current-carrying ablation electrode. The wire was aligned with B_0 and immersed in 2.5 mM NiCl_2 . The return current was carried on a wire approximately 5cm away. Both sequences used a 3D stack-of-EPI readout with 16 echoes, TR = 500 ms, $0.47 \times 0.47 \text{ mm}^2$ in-plane resolution and 5 mm slice thickness. The scan times were 4.6 min for the DAM and 2.8 min for APP. To evaluate the accuracy of both methods, the expected fields were simulated assuming two infinite length wires carrying oppositely directed current, representing the wire in the image and the return wire.

Results: *Off-resonance experiment:* The B_1 maps of the surface coil (Fig. 1) show strong fields next to the coil and a sharp drop-off away from the coil, as expected. The two techniques produce similar results and have similar SNR. The B_0 map (Fig. 2, right) shows the linear ramp of field variation caused by the y-shim. No shim was performed prior to the strong y-shim, so there is additional B_0 variation, as seen in a B_0 map on the left of Fig. 2.

Wire experiment: The B_1 maps from the current in the wire (Fig. 3) show strong fields near the wire that drop off rapidly. This is seen in the images from each technique as well as the calculated fields. The fields are stronger on the left side of the image due to the fields from the return wire. For greater detail, a cross section of the fields is plotted in Fig. 4. Both experimental methods match the simulated fields up to 1.6 G (6.8 kHz), the limit of the effective range of each technique. Above this range, the DAM has aliasing in the reconstruction, incorrectly showing fields within the effective range. The APP technique loses accuracy but still shows a monotonic increase of $|B_1|$, indicating that the values are out of range.

Conclusions: The APP technique is useful for applications requiring high-dynamic range B_1 mapping or simultaneous B_1 and B_0 mapping. Its accuracy is qualitatively similar to the DAM in 40% less imaging time. The adiabatic pulse can be optimized to trade off sensitivity to relaxation, SNR, and dynamic range in both B_1 and B_0 . Future development will involve optimization for typical relaxation times *in vivo* and further compensation for relaxation.

References: [1] R. Stollberger et al, Proc 7th SMRM, p 106, 1988; [2] V. Yarnykh, Magn. Reson. Med. 57:292, 2007; [3] K. Shultz et al, Proc 16th ISMRM, p. 1245, 2008; [4] K. Ugurbil et al, J. Magn Reson. 80:448,1988; [5] C. Cunningham et al, Magn. Reson. Med. 55:1326, 2006.

Acknowledgement: This work partly supported by NIH R01 EB008108, NIH R21 EB007715, NIH R01 EB005307.

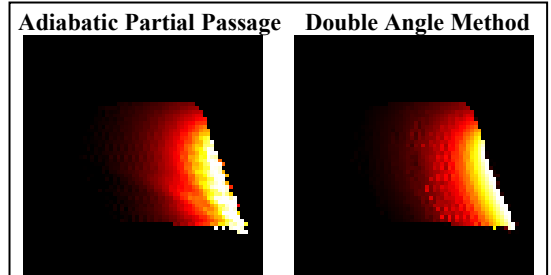


Figure 1: APP and DAM B_1 maps of phantom with strong B_0 inhomogeneity. The B_1 images are scaled from 0.1 to 1.6 Gauss (426 Hz to 6.8 kHz), the effective range of both techniques as implemented here.

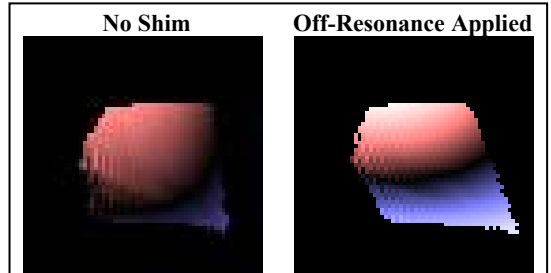


Figure 2: B_0 map of off-resonance experiment with no shim (left) and strong y-shim (right). Color indicates the sign of ΔB_0 . The observed field variation with the shim is a combination of a linear ramp in y and the variation observed with no shim. The distortion in the image with the shim, due to the applied off-resonance and the long EPI readout, can be corrected with the measured B_0 .

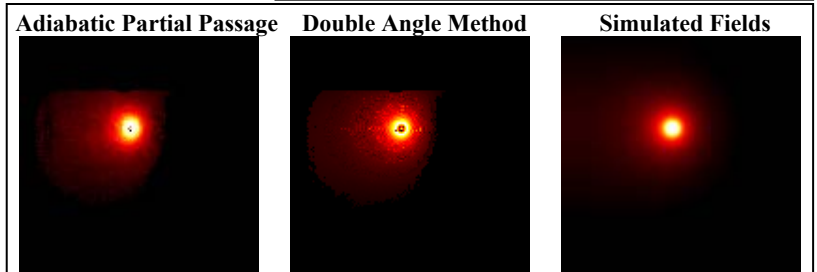


Figure 3: B_1 maps for wire phantom. There are strong fields near the wire that decay rapidly. The DAM exhibits aliasing and inaccurately reconstructs low fields very close to the wire. Otherwise, the methods agree and match the expected fields from the simulation.

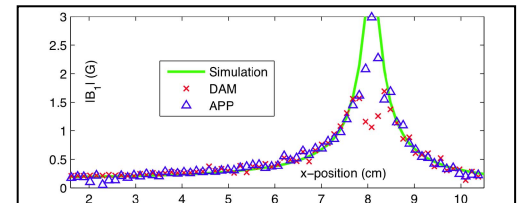


Figure 4: Cross section of B_1 maps for wire phantom. Both techniques agree well and match the simulation. At high $|B_1|$, where the field strength is beyond the effective range of both techniques, the DAM exhibits aliasing, while the APP technique shows that the values are out of range.